

Structure and magnetism in thin films and multilayers of hexagonal ruthenium and iron

D. Spišák, R. Lorenz, and J. Hafner

Institut für Materialphysik and Center for Computational Materials Science, Universität Wien, Sensengasse 8/12, A-1090 Wien, Austria

(Received 5 July 2000; published 12 February 2001)

The results of *ab initio* calculations for the electronic structure and the magnetic moments of unsupported hexagonal thin Ru and Fe films, bulk Ru and Fe metals, and Ru₅Fe₅ multilayer are presented with the focus on the crystallographic phase stability of the Fe layers. The calculated equilibrium lattice parameters of hcp Ru and Fe solids reproduce accurately the values found experimentally. For Ru/Fe multilayers it is demonstrated that in an Fe part of a multilayer an unusual hexagonal stacking with a distorted bcc-like local environment is more stable than the standard hexagonal close-packed stacking. The same result was obtained in thin Fe films and it is shown to be associated with band structure effects of Fe at the Fermi level. For thin films the ground state lattice parameters and magnetic states of films up to four monolayers were determined by total energy minimization. The faults in hexagonal planes stacking and interdiffusion do not lead to nonmagnetic Fe layers at the interfaces which were observed experimentally.

DOI: 10.1103/PhysRevB.63.094424

PACS number(s): 75.70.Cn, 71.15.Pd

I. INTRODUCTION

Among 3*d* metals iron reveals the richest structural and magnetic phase diagram. In addition to the ferromagnetic body centered cubic (bcc) α -phase iron assumes a paramagnetic face centered cubic (fcc) γ phase at temperatures above 1186 K or a nonmagnetic hexagonal close-packed (hcp) ϵ phase under a pressure of more than approximately 130 kbar. Due to advances in deposition techniques both these metastable phases could be stabilized also under normal conditions if thin Fe films were grown on appropriate substrates. γ -Fe, which can be grown on Cu(001) or Co/Cu(001) buffers, attracted much experimental¹⁻³ and theoretical⁴⁻⁷ attention in the past years because of its interesting magnetic properties. Fe atoms were shown to adopt an expanded hcp structure on Re(0001) (Ref. 8) or Ru(0001) (Ref. 9-12) substrates despite a large lattice mismatch. The remarkable conclusion was that hcp Fe in Re/Fe and Ru/Fe multilayers can exist in a ferromagnetic state. The very recent study by Perjeru *et al.*⁸ has shown that Re/Fe multilayers with a constant Fe layer thickness of 8 Å and an increasing Re layer thickness undergo a phase transition from a coherent body centered tetragonal (bct) structure with (001) plane ordering to a hcp structure at a Re layer thickness of 9 Å. The transition has no effect on the Fe magnetic moment, which is roughly $2.2\mu_B$ in both the bct and hcp phases. The atomic separations of hcp Re are expanded by about 3% with respect to hcp Ru. A similar abrupt transition from a bct to a multidomain hcp structure has been reported for Ru/Fe multilayers at a Ru layer thickness of 3.5 Å and a constant thickness of the Fe layers of 7.5 Å (Ref. 9). The structural transition is accompanied by the disappearance of magnetization. Baudelet *et al.*¹⁰ proposed a model of the structure that fits their diffraction and x-ray-absorption results on Ru/Fe, in which instead of the regular *ABAB* hcp packing with the atoms of the *B* plane occupying the threefold hollow positions above the *A* plane, an *AB'AB'* stacking with the *B'* plane translated so that the atoms in the *B'* plane take one of three bridge places above the *A* plane. This stacking leads to a face centered orthorhombic structure with the estimated lattice spacings $a_{Fe} = 2.73 \pm 0.03$ Å, $c_{Fe}/a_{Fe} = 1.55$, and $b_{Fe} = \sqrt{3}a_{Fe}$. This

structure will be referred to as the hexagonal packed (hp) structure in the present paper. The local environment of an atom in the hp structure resembles a bcc ordering along the [110] direction. Such a model can explain the anisotropy of the x-ray-absorption spectra obtained with polarization of x-ray beam parallel and normal to the *c* axis. If in addition an averaging over all three types of domains related to three possible bridge positions is considered, then also the global sixfold symmetry seen in the diffraction spectra is recovered. However, more recent extensive investigations of Ru/Fe multilayers using x-ray diffraction¹¹ are at variance with the structural model sketched above and they seem to support the regular hcp stacking with the parameters $a_{Fe} = a_{Ru} = 2.689$ Å (cf. $a_{Ru} = 2.706$ Å of the elemental Ru crystal), $c_{Fe} = 4.11$ Å and $c_{Ru} = 4.33$ Å. At higher thicknesses the hexagonal phase of the Fe layers relaxes to the more stable bcc one at a critical thickness ranging from 5 to 10 monolayers (ML), depending on the Fe layer growth rate.^{11,12}

Magnetic measurements^{9,10} detected the existence of two nonmagnetic Fe layers at both Ru/Fe and Fe/Ru interfaces. Beyond 4 ML each additional plane bears a magnetic moment of about $2.1\mu_B$ per Fe atom in a ferromagnetic (FM) alignment. Theoretical studies devoted to Ru/Fe multilayers assumed either a perfect hexagonal^{13,14} or a hp structure.¹⁵ It was concluded that while in the hcp lattice antiferromagnetic (AFM) or ferrimagnetic configurations are always preferred, the hp lattice stabilizes a FM state in Ru₃Fe₃ and Ru₅Fe₅ multilayers. The calculations failed to confirm the existence of magnetically dead Fe layers, which was explained by a weak hybridization between isoelectronic Ru and Fe elements.

In response to these controversial facts we carried out a systematic theoretical investigation of thin free-standing hexagonal Ru and Fe films, elemental Ru and Fe metals and of a Ru₅Fe₅ multilayer in hcp and hp geometries and in various magnetic states. As a further step toward a realistic modeling of atomic structures an interlayer relaxation was performed either by calculation of interatomic forces or by minimization of total energies. Furthermore, the effects of interdiffusion and stacking faults, which may not be ruled out during growth of Fe layers sandwiched by Ru layers, were explored.

II. METHODOLOGY

Our calculations were performed using the Vienna *ab initio* simulation package VASP.¹⁶ VASP finds a variational solution of the Kohn-Sham equations of density functional theory in a projector augmented-wave representation,^{17,18} using electron and spin densities based on all-electron orbitals, via a band-by-band residuum-minimization method. The projector augmented-wave potentials were constructed using scalar-relativistic Kohn-Sham equations. Exchange and correlation effects were described by the functional due to Perdew and Zunger,¹⁹ employing the spin-interpolation proposed by Vosko *et al.*²⁰ and adding generalized gradient corrections due to Perdew *et al.*²¹ The free-standing films were modeled by slabs consisting of one to four atomic layers. The periodically repeated slabs were separated by 9 (8) vacuum layers for 1 (2 and 4) ML films. Brillouin-zone integrations were performed on a Monkhorst-Pack $16 \times 16 \times 3$ grid, corresponding to 60 or 81 irreducible k points for one and two monolayer films, respectively, and on a $14 \times 14 \times 2$ grid, corresponding to 64 irreducible k points for four monolayer films. A modest Methfessel-Paxton smearing²² of the energy eigenvalues with $\sigma=0.2$ eV was applied. Calculations for Ru_5Fe_5 superlattices were run using the $10 \times 10 \times 2$ grid leading to 28 or 62 irreducible k points for the hcp and hp structures, respectively. A plane-wave energy cutoff of 300 eV was used leading to a basis set of about 150 plane waves per atom. For the ground state solution a multilayer relaxation using a conjugate-gradient algorithm and the analytical Hellmann-Feynman forces acting on the atoms was carried out.

III. RESULTS

A. Magnetism of unsupported ruthenium films

Ruthenium is a good example of a nonmagnetic solid which, when grown on an appropriate substrate such as Ag(001) or Au(001), is predicted to assume a quite large magnetic moment of about $1.7\mu_B$.^{23–25} However, no trace of magnetism for these systems has been detected in experiments. The only magnetic Ru overlayer observed so far is formed on the (0001) surface of carbon.²⁶ Because the overlap of the Ru $4d$ bands with energy bands of substrates such as Ag, Au, or C lying well below the Fermi level is rather weak, the magnetic state of a free-standing film is likely not to change dramatically from its magnetic state in a related overlayer. The magnetic moment of a free-standing Ru monolayer has been predicted to increase by 35% beyond its value in Ru/Ag(001).²³ In Fig. 1 the magnetic moments and the total energies for all possible symmetric magnetic configurations of hexagonal 1, 2, and 4 ML Ru films are shown against a wide range of interatomic spacing. In the present paper we assume always a parallel orientation of moments within a layer. The local magnetic moments are evaluated inside each muffin-tin sphere with the radius 1.3 Å for Fe and 1.4 Å for Ru atoms. The calculated equilibrium bond length in the Ru monolayer $a_{\text{Ru}}=2.55$ Å is only 3.2% higher than the in-plane nearest neighbor distance in graphite $a_{\text{C}}=2.47$ Å (Ref. 27), so the condition for an epitaxial

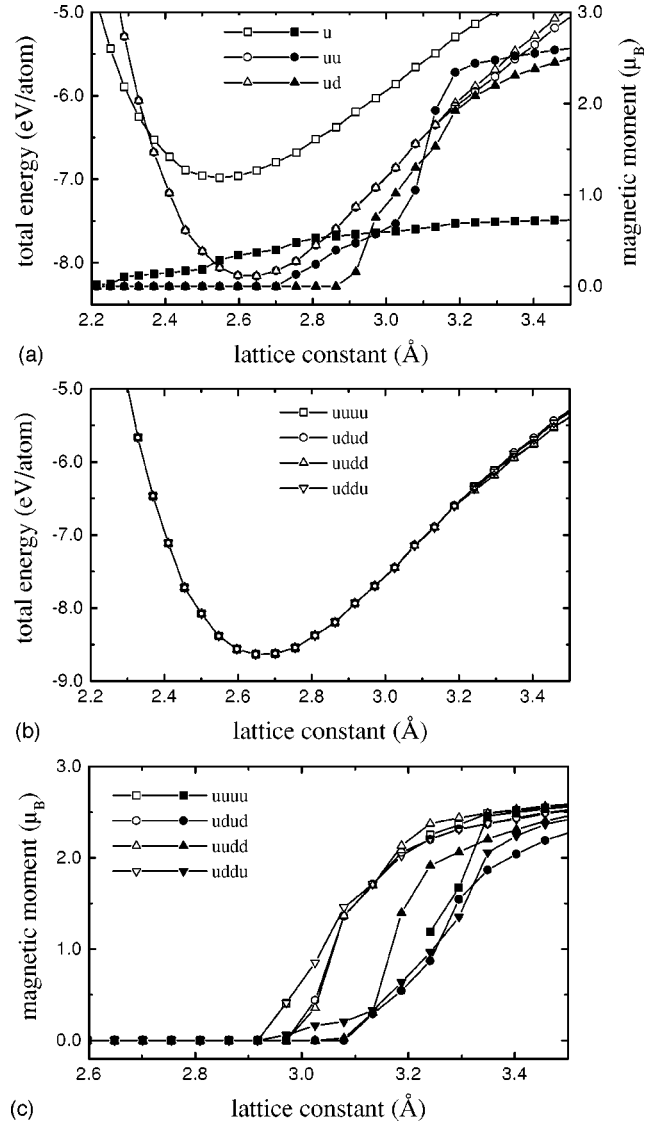


FIG. 1. Calculated total energies and magnetic moments of hexagonal (a) 1 and 2 ML thick unsupported Ru films (total energies: open symbols, magnetic moments: full symbols), (b) total energies, and (c) magnetic moments (open symbols: surface moments, full symbols: interior moments) of a 4 ML Ru films as a function of interatomic spacing. The symbols u and d in the graph legends stand for the up and down orientation of magnetic moments in a layer.

growth is met safely. This might be an important factor for producing high quality Ru/C(0001) samples in which Ru magnetism was found, even though a small magnetic moment of Ru monolayer, $\mu_{\text{Ru}}=0.28\mu_B$ was calculated. In a dilated monolayer the magnetic moment reaches slowly a value of $0.73\mu_B$, which is considerably lower than the magnetic moment of about $1.7\mu_B$ of Ru atoms arranged in a square lattice with comparable interatomic distances. This corroborates nicely the previous observations that, due to larger extent of the valence d -wave functions, the magnetic state of Ru atoms is very sensitive to their local environment. In this case an increase of the number of nearest neighbors from 4 to 6 reduces magnetic moment significantly.

In thicker films with still larger coordination numbers the nonmagnetic solutions are the most stable. The same conclusion was drawn for a bilayer Ru on Ag(001), in which the magnetic moment disappears completely.²⁵ Neglecting the possible interlayer relaxation, the calculated equilibrium distances are 2.64 and 2.66 Å for the hcp 2 and 4 ML thin films, respectively. In the case of a bilayer a ferromagnetism appears above 2.70 Å, a less stable antiferromagnetic state develops above 2.90 Å. In 4 ML films the first magnetic state is obtained for yet larger distances. Here, the FM configuration together with a bilayer AFM configuration [sequence *uudd*, *u* (*d*) stands for up (down) direction of a magnetic moment] are the preferred solutions at very large distances ($a_{\text{Ru}} > 2.95$ Å), with magnetic moments reaching $2.6\mu_B$. We note also that the FM solution could be obtained only for expanded lattices beyond $a_{\text{Ru}} = 3.24$ Å. In all configurations magnetism is strongly enhanced in the surface layers compared to the interior of the films, surface magnetism also develops at interatomic distances where inner layers are still nonmagnetic and the surface moments grow faster. A striking result is that the magnetic energy differences of all investigated configurations are exceedingly small of the order of 10 meV/atom.

B. Magnetism of unsupported iron films

The same film thicknesses and magnetic configurations as for Ru films were considered also for Fe films. As could be expected, the solutions with spontaneous magnetization are always preferred. Figure 2 presents the dependence of the total energy and the magnetic moment of 1, 2, and 4 ML unsupported Fe layers on the lattice constant. The calculated lattice constant of 2.41 Å and the magnetic moment $\mu_{\text{Fe}} = 2.62\mu_B$ in Fe monolayer compare excellently with the values reported by Moroni *et al.*²⁸ obtained by VASP employing ultrasoft pseudopotentials for describing valence states. Moreover, they found a FM coupling to be favored over an in-plane AFM coupling. As far as the 2 ML film is concerned, the energy minimum is found for the antiparallel coupling at $a_{\text{Fe}} = 2.41$ Å with the corresponding magnetic moment of $1.52\mu_B$. The FM order induces an internal tension in film with a tendency to a higher lattice constant of 2.51 Å. This value is just above a sharp transition from a low-spin to a high-spin state. The energy of the high-spin solution lies 22 meV/atom above the energy of the AFM ground state. The second, low-spin metastable FM solution at $a_{\text{Fe}} = 2.38$ Å is 49 meV/atom higher than that for the AFM state.

At intermediate distances in 4 ML Fe films neither a FM nor a bilayer AFM configurations could be obtained. The lowest energy solution was achieved for a ferrimagnetic state with parallel inner moments of $0.43\mu_B$ coupled antiparallel to the outer moments of $1.66\mu_B$ at the equilibrium lattice constant of 2.43 Å. However, at elevated interatomic distances more than 2.59 Å the FM configuration settles down. In relation to Ru/Fe multilayers we considered also a FM hp geometry as seen in Figs. 2(b), 2(c). Now magnetism appears at much smaller lattice constants and the ground state [$a_{\text{Fe}} = 2.55$ Å, the surface and subsurface moments are $\mu_{\text{Fe}}(S) = 2.64\mu_B$, $\mu_{\text{Fe}}(S-1) = 2.49\mu_B$] lies 5 meV/atom lower than that of the ferrimagnetic state of hcp phase. If the interatomic distances are expanded any further, the moments saturate to about $3.2\mu_B$ independent of film thickness and structure.

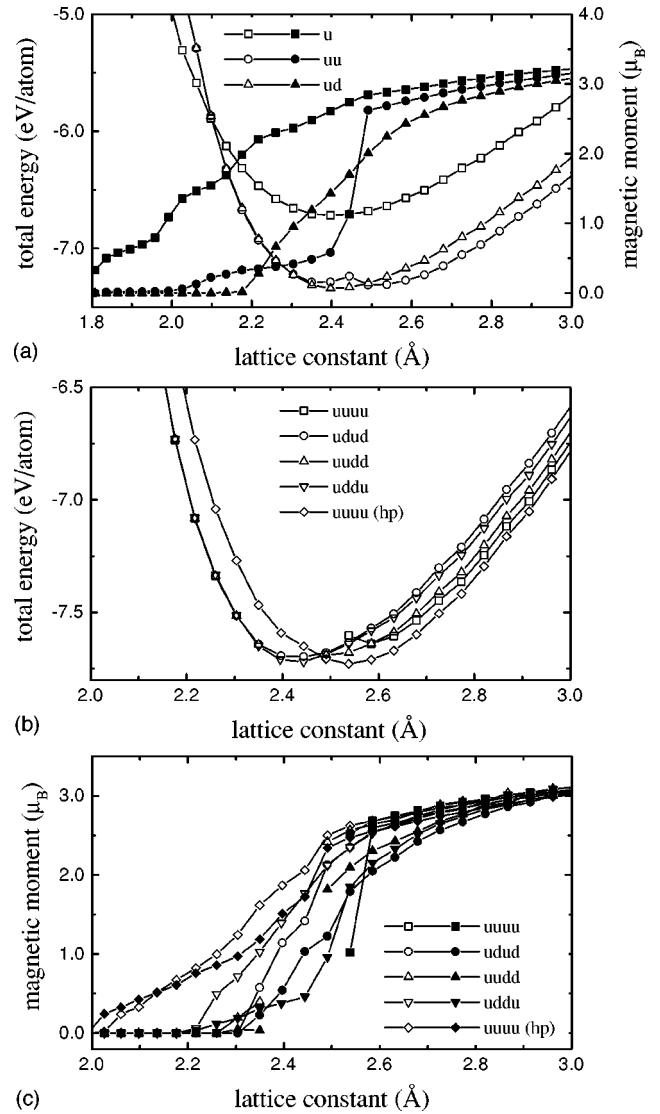


FIG. 2. Calculated total energies and magnetic moments of hexagonal close-packed (a) 1, 2 and (b), (c) 4 ML thick unsupported Fe films. For symbols meaning see caption of Fig. 1. In plots (b), (c) additional results for FM hexagonal packed geometry are included (diamond symbols).

$= 2.64\mu_B$, $\mu_{\text{Fe}}(S-1) = 2.49\mu_B$] lies 5 meV/atom lower than that of the ferrimagnetic state of hcp phase. If the interatomic distances are expanded any further, the moments saturate to about $3.2\mu_B$ independent of film thickness and structure.

C. Pure hexagonal ruthenium and iron

In this section we wish to take a look at structural and magnetic properties of elemental Ru and Fe solids. The experimentally determined hexagonal Ru lattice parameters are $a_{\text{Ru}} = 2.706$ Å, $c_{\text{Ru}} = 4.282$ Å,²⁷ thus the axial ratio $c/a = 1.582$ is somewhat reduced from the ideal value of 1.633. The calculated lattice constant a_{Ru} is 2.70 Å (see Fig. 3) if the c/a ratio is fixed to the ideal value. If the distortion is optimized as well we get $a_{\text{Ru}} = 2.73$ Å, $c/a = 1.58$ in very

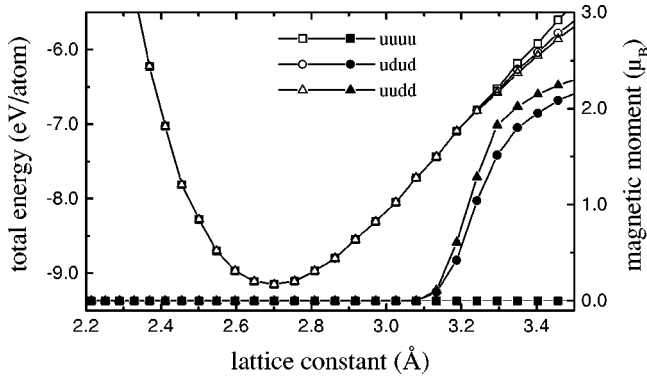


FIG. 3. Calculated total energies (open symbols) and magnetic moments (full symbols) of bulk hcp Ru against lattice constant.

good agreement with experimental data. The smooth onset of magnetism begins at large interatomic distances 3.1 \AA and the favored magnetic order is a bilayer AFM sequence. It is well known that the most favorable conditions for antiferromagnetism are expected for $3d$ and $4d$ transition metals with nearly half-filled d bands. It turns out that, in contrast to thin films, the FM phase of a hcp Ru solid could not be found in our calculations for any lattice spacing up to 3.5 \AA .

Because the structure of Fe as a part of Ru/Fe superlattices is known to undergo significant deformations we performed a structure optimization by varying both a and c lattice parameters. The calculated equilibrium values $a_{\text{Fe}} = 2.44 \text{ \AA}$, $c_{\text{Fe}} = 3.90 \text{ \AA}$ ($c_{\text{Fe}}/a_{\text{Fe}} = 1.60$) which were obtained for a nonmagnetic state, reproduce convincingly the experimental data, $a_{\text{Fe}} = 2.46 \text{ \AA}$, $c_{\text{Fe}} = 3.94 \text{ \AA}$ ($c_{\text{Fe}}/a_{\text{Fe}} = 1.60$) of the hcp ϵ phase.²⁷ The calculated bulk modulus of 2.82 Mbar allows us to estimate the lattice compression at 130 kbar , the pressure upon which the experimental data was obtained. The reduction of lattice constants lies below 1.5% . From the Fig. 4, depicting a volume variation of the total energies and magnetic moments for FM, single AFM and bilayer AFM configurations at $c/a = 1.633$, it is obvious that the energy minimum is located exactly at the border of nonmagnetic-antiferromagnetic transition. In this context we recall that disordered RuFe alloys with less than 30% Ru, which have an atomic volume expanded by about 5% with respect to high-pressure hcp Fe, do exhibit antiferromagnetism.²⁹ At the in-plane lattice spacing corresponding to that of Ru and generally for all in-plane distances above 2.58 \AA , provided $c/a = 1.633$, a FM order is stabilized. Of course, at enlarged in-plane distances the axial ratio tends to decrease. Fig. 5 displays the dependence of total energies and magnetic moments of hcp Fe on the c/a ratio when its in-plane spacing is kept at $a_{\text{Ru}} = 2.70 \text{ \AA}$. The axial ratio drops to 1.49 , but it should be noticed that the volume per atom is about 27% in excess of the calculated equilibrium hcp Fe volume 10.1 \AA^3 . Complete contour plots of the total energy as a function of a and c/a for FM, single AFM and bilayer AFM ordering are given in Fig. 6. The AFM configurations reveal a similar topology of the total energy surface which can be characterized as slightly distorted quadratic form. For varying c/a , the energy at minimum does not follow the path of constant volume repre-

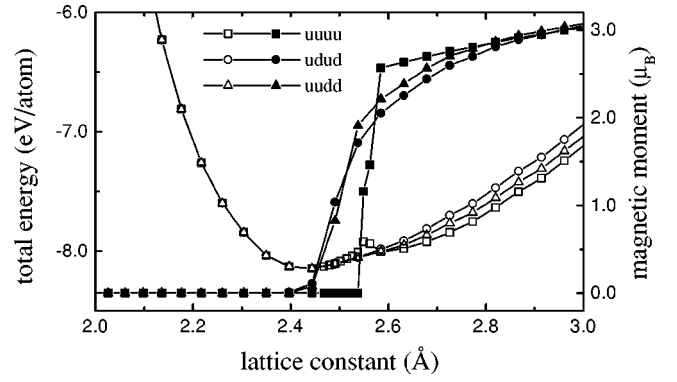


FIG. 4. Calculated total energies (open symbols) and magnetic moments (full symbols) of hcp bulk Fe against lattice constant.

sented by the dashed line in Fig. 6, rather both contraction and expansion along the c axis lead to increased equilibrium volumes in order to eliminate the shortest interatomic bonds. For the FM phase with more complex topology of energy surface we found a secondary minimum, visible also in Fig. 4, corresponding to a perfect hcp stacking with a total energy higher by 150 meV/atom with respect to the ground state.

The main aim of this work concentrates on the structure of Fe part in Ru/Fe multilayers. To this end, it is useful to investigate also the magnetic properties of bulk hp Fe. A full structural optimization of FM hp Fe predicts $a_{\text{Fe}} = 2.562 \text{ \AA}$, $c_{\text{Fe}}/a_{\text{Fe}} = 1.612$, and $\mu_{\text{Fe}} = 2.41 \mu_B$, for a bilayer antiferromagnetic hp phase we find $a_{\text{Fe}} = 2.482 \text{ \AA}$, $c_{\text{Fe}}/a_{\text{Fe}} = 1.711$, and $\mu_{\text{Fe}} = 2.02 \mu_B$, and for a single layer AFM state the equilibrium parameters are $a_{\text{Fe}} = 2.459 \text{ \AA}$, $c_{\text{Fe}}/a_{\text{Fe}} = 1.734$, and $\mu_{\text{Fe}} = 1.69 \mu_B$. Thus, as in γ -Fe, the FM phase is connected with the largest atomic volume, but unlike to γ -Fe with a bilayer AFM ground state⁷ found in the collinear setup, in the hp Fe the bilayer and single layer AFM solutions have a energy higher by 99 and 184 meV/atom with respect to a FM ground state solution. From the comparison of the results for hcp (Fig. 4) and hp (Fig. 7) stacking (both calculated at the ideal c/a ratio) three obvious conjectures can be made. Firstly, a smooth onset of magnetism in the hp phase occurs at much smaller volumes than in the hcp phase. Secondly, the energy of the nonmagnetic hcp structure with

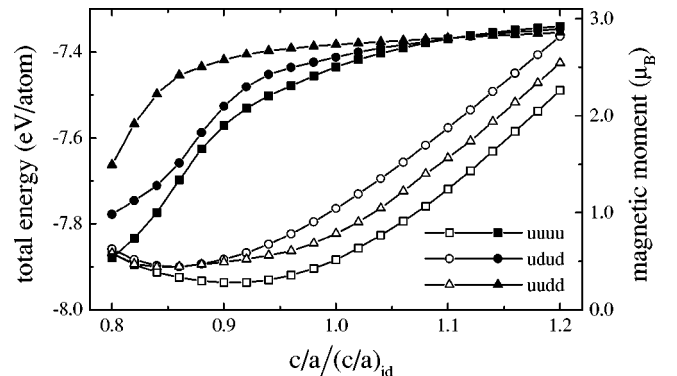


FIG. 5. Dependence of total energies (open symbols) and magnetic moments (full symbols) of hcp Fe with in-plane lattice constant of Ru on the axial ratio c/a .

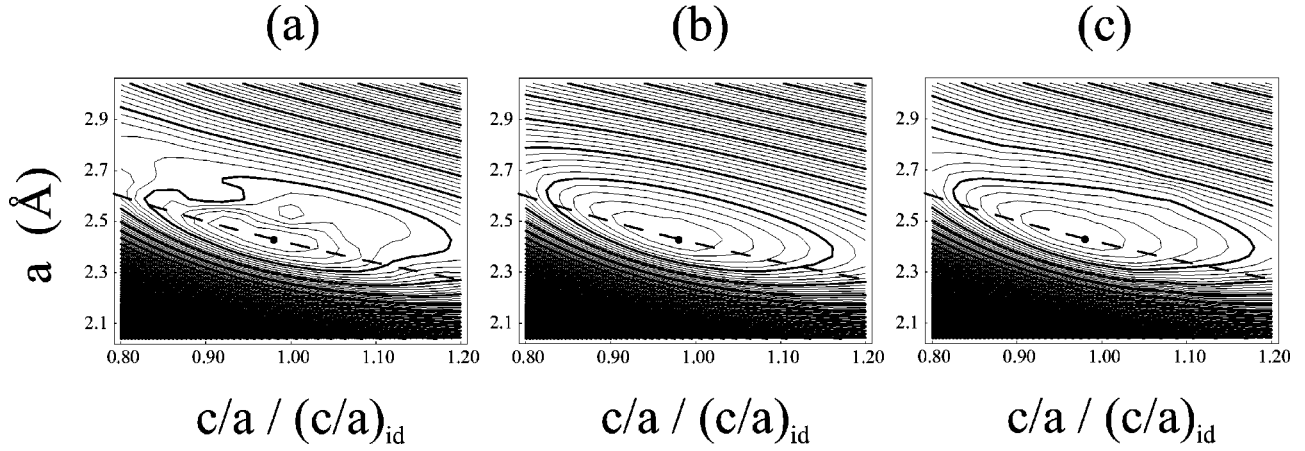


FIG. 6. Contour plots of total energy $E(a, c/a)$ for (a) FM, (b) single layer AFM, and (c) bilayer AFM hcp Fe. The contour interval is 40 meV (0.2 eV between bold lines), the minimum in the total energy is marked by a full dot. The dashed curves denote the paths of constant volume.

smaller volume is lower than that of the larger volume ground state of FM hp structure, $\Delta E = 39$ meV/atom. Thirdly, if the lattice constant is increased over 2.53 Å, the FM hp solution is more stable than the hcp solution and the total energies of both ferromagnetic hcp and hp phases follow nearly the same curve shifted by some 60 meV/atom. This indicates that if the in-plane Fe lattice constant is strained to the Ru lattice constant, the hp geometry can be preferred over the hcp geometry.

D. Ru/Fe multilayers

In order to investigate a potential departure from ideal hcp stacking in Fe layers sandwiched by Ru, a Ru_5Fe_5 multilayer was chosen as a representative system. All in-plane lattice spacings were fixed at the calculated value $a_{\text{Ru}} = 2.70$ Å, a perfect hcp structure of the Ru layer was assumed and the Fe layers were built either as hcp $ABABA$ succession of hexagonal planes or as hp $AB'AB'A$ sequence with shifted B' planes. The interlayer distances in the Fe layer could vary. The Ru-Fe interlayer distances were taken as an average of the distances in Ru and Fe layers. Table I lists the total energy differences and layer magnetic moments for two val-

ues of $c_{\text{Fe}}/a_{\text{Ru}} = 1.633$ (corresponding to the ideal hcp geometry) and 1.490 (corresponding to the energy minimum of bulk hcp Fe strained to the in-plane lattice constant of Ru). For the case of coherent hexagonal geometry ($c_{\text{Fe}}/a_{\text{Ru}} = 1.633$) the calculations were carried out allowing for all possibilities leading to a symmetric alignment of Fe moments around the central Fe layer. Because an AFM order (ududu configuration) was found to be energetically extraordinarily disadvantageous, it was excluded from further calculations. The effect of a relaxation of the Fe interlayer distances along the [001] direction, shown in Fig. 8, is to stabilize a FM hp structure with $c_{\text{Fe}}/a_{\text{Ru}} = 1.48$. This value is in reasonable agreement with values of $c_{\text{Fe}}/a_{\text{Ru}} = 1.55$ (Ref. 10) or 1.52 (Ref. 11), estimated from x-ray diffraction experiments. The most stable magnetic ordering in both phases is the FM order with average moments of about $2.71\mu_B$ for the ideal $c_{\text{Fe}}/a_{\text{Ru}}$ ratio and $2.54\mu_B$ in multilayers with $c_{\text{Fe}}/a_{\text{Ru}} = 1.49$. In Ru layers non-negligible moments were obtained only in the interface layer, with a magnitude of $0.18\mu_B$ and an antiparallel orientation with respect to adjacent Fe moments.

In the next step we carried out a full structural relaxation of interlayer distances in Ru_5Fe_5 multilayer with the total volume as a free parameter. The relaxation yields the following interlayer distances (I stands for interface layer): $d_{\text{Ru,Ru}}(I, I-1) = 2.150$ Å, $d_{\text{Ru,Ru}}(I-1, I-2) = 2.168$ Å, in the Ru layer, $d_{\text{Fe,Fe}}(I, I-1) = 1.974$ Å, $d_{\text{Fe,Fe}}(I-1, I-2) = 1.997$ Å, in the Fe layer and $d_{\text{Ru,Fe}}(I, I) = 2.086$ Å at the interface. It can be concluded that the crystallographic structure in Ru and Fe layers is homogeneous with average axial ratios $c_{\text{Fe}}/a_{\text{Ru}} = 1.47$ and $c_{\text{Ru}}/a_{\text{Ru}} = 1.60$.

The physical origin of the preference for a hp geometry over a standard hcp one can be explained in terms of the layer projected densities of states, which are presented in Fig. 9. The majority densities of states of the hcp phase are characterized by three pronounced peaks related to bonding, nonbonding and antibonding states. These states are almost completely filled and the states of inner layers are scarcely affected by interaction with electronic states of Ru. The mi-

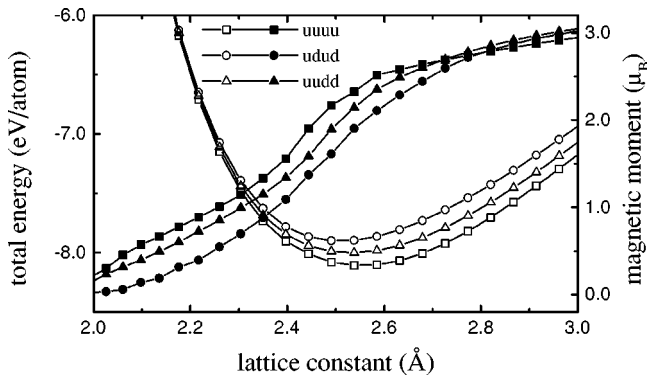


FIG. 7. Calculated total energies (open symbols) and magnetic moments (full symbols) of hexagonal packed bulk Fe as a function of lattice constant.

TABLE I. Total energy differences ΔE and magnetic moments μ_{Fe} of interface (I), second interface ($I-1$), and middle ($I-2$) Fe layers of the Ru_5Fe_5 multilayer with Fe part of multilayer forming a hcp or hp lattice.

Magn. conf.	ΔE (meV/atom)		$\mu_{\text{Fe}}(I)$ (μ_B)		$\mu_{\text{Fe}}(I-1)$ (μ_B)		$\mu_{\text{Fe}}(I-2)$ (μ_B)	
	hcp	hp	hcp	hp	hcp	hp	hcp	hp
$c_{\text{Fe}}/c_{\text{Ru}}=1.633$								
uuuuu	0	0	2.59	2.60	2.75	2.73	2.75	2.71
udddu	22	50	2.39	2.42	-2.64	-2.67	-2.73	-2.73
uuduu	24	52	2.62	2.65	2.66	2.70	-2.47	-2.40
ududu	48	127	2.42	2.47	-2.54	-2.66	2.51	1.42
$c_{\text{Fe}}/c_{\text{Ru}}=1.490$								
uuuuu	0	0	2.37	2.38	2.63	2.56	2.62	2.55
udddu	11	53	1.84	2.00	-2.37	-2.45	-2.58	-2.58
uuduu	36	60	2.40	2.43	2.38	2.44	-1.91	-2.05

minority densities of states have essentially the same character with the nonbonding peak falling almost exactly at the Fermi level. On the other hand, the electronic density of states of the hp phase shows a bimodal structure (similar to that in bcc metals) with a wide bonding-antibonding pseudogap in the central Fe layer, which disappears in the interface layer for the majority states. In contrast, for the minority states the pseudogap exists also in the interface layer. This large disparity in the minority densities of states accounts for the differences in total energies between the hcp and hp geometries—the density of states at Fermi level is nearly doubled in the hcp lattice, resulting in an increase of the band energy.

The next point to be discussed is how a misalignment in the hexagonal stacking, which is conceivable to happen, depending on preparation method and conditions, could influence the structural and magnetic properties. Our results for several stacking faults, taking $c_{\text{Fe}}/a_{\text{Ru}}=1.49$, are summarized in Table II. The shifted planes (A' , B') were always moved in the same direction. More complicated combinations consisting of planes translated along any of three pos-

sible lateral directions are not expected to provide any noteworthy deviations. From the values in Table II it is obvious that the magnetic state is insensitive to structural misalignment, but not the energies. At the Ru/Fe interface an Fe plane continues to grow in the standard hcp stacking but further Fe layer prefers to adopt a shifted position. To put it another way, the $AB'AB'$ sequence is stable only in the interior of Fe layer. Any deviation from this stacking costs an energy of at least ~ 20 meV/atom. The least probable are

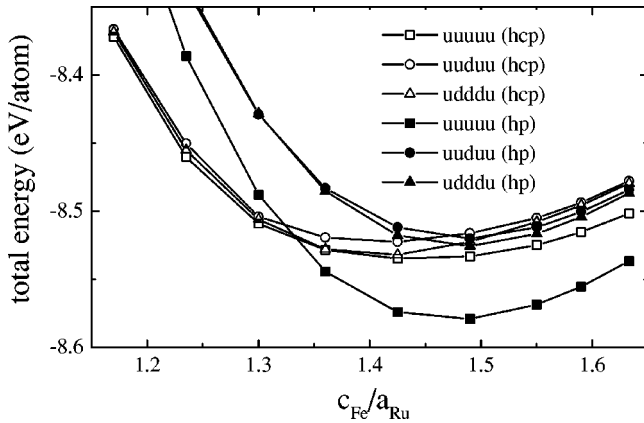


FIG. 8. Dependence of total energies in Ru_5Fe_5 multilayer on axial distortion in Fe layer. The structure of Fe layer is hcp (open symbols) or hp (full symbols).

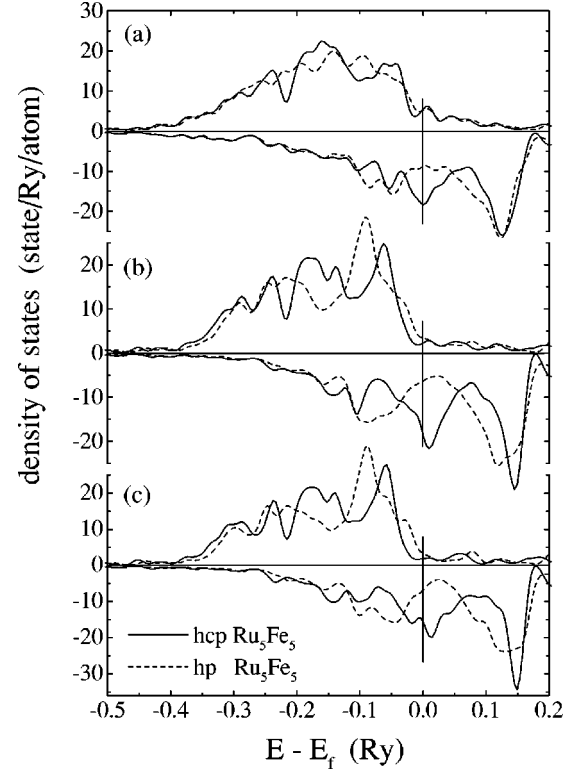


FIG. 9. Layer resolved densities of states in (a) interface, (b) second, and (c) central Fe layers of Ru_5Fe_5 multilayer with $c/a = 1.49$. The structure of Fe layers is hcp (solid lines) or hp (dashed lines).

TABLE II. Total energy differences ΔE and magnetic moments μ_{Fe} of the ferromagnetic Ru_5Fe_5 multilayer with axial ratio $c_{\text{Fe}}/c_{\text{Ru}}=1.49$ for different stacking of hexagonal planes in the Fe layer.

Stacking	ΔE (meV/atom)	$\mu_{\text{Fe}}(I)$ (μ_B)	$\mu_{\text{Fe}}(I-1)$ (μ_B)	$\mu_{\text{Fe}}(I-2)$ (μ_B)
$AB'AB'A$ (hp)	0	2.38	2.56	2.55
$AB'ABA$	23	2.39	2.57	2.61
$ABABA$ (hcp)	46	2.37	2.63	2.62
$A'BA'BA'$	82	2.42	2.55	2.57
$ABA'BA$	90	2.40	2.55	2.42
$A'BABA'$	104	2.43	2.60	2.64

stacking faults just at the Ru/Fe interface. Interestingly, in these configurations ($A'BA'BA'$, $A'BABA'$) small Ru interface magnetic moments $\sim 0.09\mu_B$ couple ferromagnetically to the adjacent Fe moments indicating that the contraction of Ru-Fe distances modifies the Ru-Fe magnetic interaction from AFM to FM.

Finally, we would like to comment on the existence of two ML thick nonmagnetic region at interfaces as reported from experimental observations. It has been suggested^{10,13} this effect comes from structural imperfections such as stacking faults, antistructure defects or lattice relaxation. We believe, in the light of our results discussed above, which reveal only a modest sensitivity of the magnetism to structural changes, that these conjectures are not justified. Another plausible explanation at hand could be interdiffusion. To explore this assumption we carried out a calculation for a FM Ru_5Fe_5 multilayer with (2×1) cell and the axial ratio $c_{\text{Fe}}/a_{\text{Ru}}=1.49$, where the layers around each interface were occupied by a $\text{Ru}_{0.5}\text{Fe}_{0.5}$ alloy. This is a simple way to model a surface roughness or interfacial mixing. It turned out that the interface Fe magnetic moments kept a large magnetic moment of about $2.2\mu_B$, so that an interdiffusion limited to a very few interatomic layers around an interface cannot lead to vanishing magnetic moments. As an eventual possibility to explain the reported ‘‘lack’’ of interface magnetism could be a more intricate magnetic structure than that investigated by us. In this respect we recall the results of Wu and Freeman³⁰ who found a row-wise in-plane AFM ground state of Fe overlayers on a hcp Ru surface. If this scenario were acceptable in Ru/Fe multilayers, it remains to be clarified, how an AFM configuration at an interface would transform abruptly into detected FM order in the interior of an Fe layer. Thus, observations of magnetic dead layers is a puzzling phenomenon deserving further theoretical and experimental attention.

IV. CONCLUSIONS

We have presented detailed *ab initio* local-spin-density calculations of the magnetic properties of the hexagonal phases of bulk Ru and Fe metals, of free-standing Ru and Fe films with up to four monolayers and of Ru/Fe multilayers represented by Ru_5Fe_5 system. In addition to the conventional hexagonal AB stacking of close-packed layers, we

have also examined an AB' stacking (the hp structure), in which the atoms in the B' layer occupy bridge sites of the A layers, leading to an overall orthorhombic symmetry. For bulk hcp Ru we find that magnetic ordering exists only at strongly expanded lattice parameters, with a bilayer AFM sequence being slightly favored over a simple layer-by-layer AFM state. A similar situation is found for hcp Fe, but here a modest expansion is sufficient to stabilize FM ordering. The transition to a FM state is abrupt, whereas antiferromagnetic arrangements develop progressively with an increasing volume. Similar to fcc iron, the potential energy surface of FM hcp Fe as a function of basal lattice constant and axial ratio has a rather complex shape, as a consequence of the existence of low- and high-spin states. In the hp phase of Fe, a FM configuration is stable even under compression. Although FM hp Fe is less stable than the nonmagnetic hcp phase at the equilibrium volume, the phase has lower energy in an expanded state.

Unsupported Ru films beyond a monolayer limit are magnetically ordered only at considerably dilated lattice constants and even then the magnetic energy differences remain very small. Fe films show a very complex behavior: Monolayers are FM ordered at equilibrium, in bilayers an AFM configuration is energetically almost degenerate with a high-spin FM phase with moderately larger equilibrium distances. In a 4 ML Fe films the hcp structure has a ferrimagnetic ground state which is higher in energy than a FM hp configuration at a bit larger volume.

These complexities are reflected in the structural and magnetic properties of Ru/Fe multilayers. Assuming an ideal hcp geometry in the Ru part of Ru_5Fe_5 multilayers, we find that a FM configuration is favored over any possible AFM order in both hcp ($ABABA$) and hp ($AB'AB'A$) structures of the Fe_5 layers, the hp structure being 46 meV/atom lower in energy compared to hcp structure. The stability of the hp phase can be explained in terms of the Fe-minority densities of states showing a minimum around the Fermi level. In the multilayers, the Fe moments are enhanced over their bulk values in the interior of the FM films and are bulklike at the Ru/Fe interface. Any induced magnetic ordering at the Ru part of the interface remains very small.

The exploration of plane stacking faults in Fe layers leads to conclusion that a misalignment from hexagonal $AB'AB'$ succession is likely to take place at higher deposition temperatures in the film interior rather than at Ru/Fe interfaces, where it costs more misfit energy, and that the magnetic moments are almost independent of this sort of structural defects.

The presented results are in good agreement with experiment concerning the structural features of the Ru/Fe multilayers reported by Baudalet *et al.*¹⁰ However, our calculations do not support the conjecture of ‘‘magnetically dead’’ Fe layers at the interface. We have also probed a possibility that an interdiffusion could lead to a quenching of magnetism. Nevertheless, it turned up that at least a 50/50 mixing in two monolayers at the interface leads only to a modest reduction of the Fe moments, so that substitutionally disor-

dered interfaces alone do not account for a lack of interface magnetism. The cause of the discrepancy might be looked for in a large lattice strain at the Ru/Fe interface, which could eventuate in more complicated structural effects in the Fe layers near the interface. This problem certainly deserves further investigations.

ACKNOWLEDGMENTS

This work has been supported by the Austrian Science Funds within Project No. P12357 “Magnetism on the nanometer scale” and by the Austrian Ministry for Science through the Center for Computational Materials Science.

-
- ¹J. Thomassen, F. May, B. Feldmann, M. Wuttig, and H. Ibach, Phys. Rev. Lett. **69**, 3831 (1992).
- ²S. Müller, P. Bayer, C. Reischl, K. Heinz, B. Feldmann, H. Zillgen, and M. Wuttig, Phys. Rev. Lett. **74**, 765 (1995).
- ³K. Heinz, S. Müller, and P. Bayer, Surf. Sci. **352-4**, 942 (1996).
- ⁴R. Lorenz and J. Hafner, Phys. Rev. B **54**, 15 937 (1996).
- ⁵T. Asada and S. Blügel, Phys. Rev. Lett. **79**, 507 (1997).
- ⁶E.G. Moroni, J. Hafner, and G. Kresse, J. Phys.: Condens. Matter **11**, L35 (1999); J. Magn. Magn. Mater. **198-199**, 551 (1999).
- ⁷D. Spišák and J. Hafner, Phys. Rev. B **61**, 16 129 (2000).
- ⁸F. Perjeru, M.M. Schwickert, Tao Lin, A. Anderson, and G.R. Harp, Phys. Rev. B **61**, 4054 (2000).
- ⁹Tao Lin, M.A. Tomaz, M.M. Schwickert, and G.R. Harp, Phys. Rev. B **58**, 862 (1998).
- ¹⁰F. Baudalet, A. Fontaine, G. Tourillon, D. Guay, M. Maurer, P. Piecuch, M.F. Ravet, and V. Dupuis, Phys. Rev. B **47**, 2344 (1993).
- ¹¹M.C. Saint-Lager, D. Raoux, M. Brunel, M. Piecuch, E. Elkaim, and J.P. Lauriant, Phys. Rev. B **51**, 2446 (1995).
- ¹²S. Andrieu, M. Piecuch, and J.F. Bobo, Phys. Rev. B **46**, 4909 (1992).
- ¹³D. Knab and C. Koenig, Phys. Rev. B **43**, 8370 (1991).
- ¹⁴D. Knab and C. Koenig, J. Magn. Magn. Mater. **93**, 398 (1991).
- ¹⁵D. Knab and C. Koenig, J. Magn. Magn. Mater. **98**, 10 (1991).
- ¹⁶G. Kresse and J. Furthmüller, Comput. Mater. Sci. **6**, 15 (1996); Phys. Rev. B **54**, 11 169 (1996).
- ¹⁷P. Blöchl, Phys. Rev. B **50**, 17 953 (1994).
- ¹⁸G. Kresse and D. Joubert, Phys. Rev. B **59**, 1758 (1999).
- ¹⁹J. Perdew and A. Zunger, Phys. Rev. B **23**, 5048 (1981).
- ²⁰S.H. Vosko, L. Wilk, and M. Nusair, Can. J. Phys. **58**, 1200 (1980).
- ²¹J.P. Perdew, J.A. Chevary, S.H. Vosko, K.A. Jackson, M.R. Pederson, D.J. Singh, and C. Fiolhais, Phys. Rev. B **46**, 6671 (1992).
- ²²M. Methfessel and A. Paxton, Phys. Rev. B **40**, 3616 (1989).
- ²³R. Wu and A.J. Freeman, Phys. Rev. B **45**, 4007 (1992).
- ²⁴S. Blügel, Phys. Rev. Lett. **68**, 851 (1992).
- ²⁵S. Blügel, Phys. Rev. B **51**, 2025 (1995).
- ²⁶R. Pfandzetter, G. Steierl, and C. Rau, Phys. Rev. Lett. **74**, 3467 (1995).
- ²⁷P. Villars and L.D. Calvert, *Pearson's Handbook of Crystallographic Data for Intermetallic Phases*, 2nd ed. (ASM International, 1991).
- ²⁸E.G. Moroni, G. Kresse, J. Hafner, and J. Furthmüller, Phys. Rev. B **56**, 15 629 (1997).
- ²⁹D.I.C. Pearson and J.M. Williams, J. Phys. F **9**, 1797 (1979).
- ³⁰R. Wu and A.J. Freeman, Phys. Rev. B **44**, 4449 (1991).